Impurity level of Co in $Pb_{1-x-y}Sn_xCo_yTe$ alloys

© E.P. Skipetrov[1], N.S. Konstantinov[1], I.V. Shevchenko[1], E.V. Bogdanov[1], L.A. Skipetrova[1], A.V. Knotko[2]

[1] Lomonosov Moscow State University (Faculty of Physics),
119991 Moscow, Russia
[2] Lomonosov Moscow State University (Faculty of Materials Science),
119991 Moscow, Russia

E-mail: skip@mig.phys.msu.ru

Received July 6, 2025
Revised November 11, 2025
Accepted November 11, 2025

The phase and elemental compositions and galvanomagnetic properties of samples from the $Pb_{1-x-y}Sn_xCo_yTe$ single crystal ingot ($x = 0.08$, $y = 0.01$) were studied. The distributions of tin and cobalt impurities along the length of the ingot were determined, and microscopic inclusions of the second phase enriched in cobalt were found at the end of the ingot. An abnormal increase in the Hall coefficient was found with increasing temperature, and in samples from the middle part of the ingot, an increase in the hole concentration and a linear increase in the Fermi energy at $T = 4.2$ K with increasing tin content were found, indicating pinning of the Fermi level by the resonant Co level located in the valence band. The position of the Co level and the compositional coefficient of its motion relative to the top of the valence band are estimated. A diagram of the rearrangement of the electronic structure of alloys with increasing tin concentration is proposed.

Keywords: $Pb_{1-x}Sn_xTe$ alloys, 3*d* transition metal impurities, galvanomagnetic properties, resonant level of Co, rearrangement of the electronic structure.

DOI: 10.61011/SC.2025.08.62603.8347

1. Introduction

The electronic structure of alloys based on lead telluride with impurities of 3*d* transition metals with variable valence, as well as galvanomagnetic, thermoelectric, and magnetic properties related to its features and parameters, have been studied for several decades. However, for a long time these studies were mainly limited to chromium-doped lead telluride [1–8], and only after the discovery in 2006 of a deep impurity level of vanadium in the band gap of PbTe [9] spread to alloys $Pb_{1-x}Sn_xTe$, $Pb_{1-x}Ge_xTe$, etc., including other impurities of this series (Sc, Ti, Cr, V, Fe, Ni).

It is currently known that in PbTe, deep levels of impurities from the beginning of the series of 3*d* transition metals (Sc, Ti, Cr) are resonant and are located high in the conduction band [10–12,1–8], the V level is located in the band gap just below the bottom of the conduction band [9,13], and the Fe and Ni levels are located in the vicinity of the top of the valence band [14,15]. The band gap in $Pb_{1-x}Sn_xTe$ alloys decreases with increasing tin concentration, and the levels of Cr, V, Fe, and Ni move downward at approximately the same speed relative to the middle of the band gap, gradually approaching the extremes of the „heavy“ valence band at points Σ of the Brillouin zone [16–19]. Therefore, the levels of Fe and Ni may intersect with the top of the Σ-band, which is moving towards them, and lead to a significant increase in the thermoelectric efficiency of alloys [20–23].

The energies of deep levels from the end of the 3*d* transition metal series (the levels of Co and Cu) in $Pb_{1-x}Sn_xTe$ alloys which, like the Fe and Ni levels and by analogy with the levels of 3*d* transition metals in $A^{III}B^{V}$ and $A^{II}B^{VI}$ semiconductors [24], may lie in the valence band are not yet known.

To experimentally detect the impurity level of Co in the electronic spectrum of $Pb_{1-x}Sn_xTe$ alloys and determine its energy position relative to the top of the valence band at points *L* of the Brillouin zone, depending on the concentration of tin in the matrix, galvanomagnetic properties were studied in this work in weak magnetic fields ($B \le 0.07$ T, $4.2 \le T \le 300$ K) of samples from single crystal ingot $Pb_{1-x-y}Sn_xCo_yTe$ ($x = 0.08$, $y = 0.01$).

2. Samples, experimental methods

A single crystal ingot of $Pb_{1-x-y}Sn_xCo_yTe$ (1199) with tin concentration $x = 0.08$ and cobalt concentration $y = 0.01$ in the initial charge was synthesized by the vertical Bridgman-Stockbarger method from a mixture pre-synthesized PbTe and $CoTe_2$ compounds. It was assumed that the choice of $CoTe_2$ with a lower melting point than Co and CoTe as a dopant would increase the solubility of the Co impurity in the matrix $Pb_{1-x}Sn_xTe$. The methods of additional purification and preparation of the initial components and compounds, as well as the modes of synthesis of a single-crystal ingot, are described in detail in Refs. [25,26].

The ingot was cut into a series of 20 washers with a thickness of ~ 1.5 mm, from which 2−3 samples with dimensions of $4.0 \times 0.7 \times 0.7$ mm were cut. The washer numbers are then used as the numbers of the tested samples.

The galvanomagnetic parameters of the samples were measured by the four-probe method at direct current in the temperature range of 4.2−300 K, in magnetic fields up to 0.07 T.

3. Experimental results and discussion

3.1. Composition of the studied samples

The distribution of tin and cobalt along the ingot was determined by X-ray fluorescence microanalysis using a LEO SUPRA 50VP scanning electron microscope. Micrographs of the chipped surfaces of the studied samples and X-ray spectra from the areas indicated in the figures are shown in Figure 1 (the numbers in the photographs correspond to the numbers of the studied samples from ingot 1199).

Practically all samples are single-phase and have good uniformity within the limits of experimental error. In addition, as in the previously studied alloys $Pb_{1-x-y}Sn_xCr_yTe$ [16] and $Pb_{1-x-y}Sn_xFe_yTe$ [25,26], microscopic inclusions of the second phase were found in a number of samples, mainly from the end of the ingot, representing single clearly defined regions with a reduced content of Pb and Sn, but enriched in Co and Te (similar in composition to the compound $CoTe_2$) (see Figure 1). It was previously shown that the presence of such inclusions, apparently associated with exceeding the solubility limit of the impurity, ensures a uniform distribution of the impurity in the main phase, which occupies almost the entire volume of the samples, and does not affect their galvanomagnetic and even oscillation parameters [16,25,26].

Just as in other doped alloys $Pb_{1-x}Sn_xTe$, in the main phase the tin concentration increases exponentially along the ingot [27,28] in the range of concentrations $x = 0.07-0.14$ (Figure 2). At the same time, the area under the tin distribution curve corresponding to the total tin concentration in the ingot $S_x \approx 0.088$ is in good agreement with the tin concentration in the initial growth charge ($x = 0.08$).

Unfortunately, the experimental values of the cobalt concentration in all samples turned out to be less than the error of their determination, which did not allow us to determine the distribution of the Co impurity along the ingot with almost the same accuracy of concentration determination as in the case of tin. However, since microscopic inclusions of the second phase enriched in cobalt were detected at the end of the ingot, and by analogy with the distribution of other impurities of 3*d* transition metals in $Pb_{1-x}Sn_xTe$ alloys, it can be assumed that the concentration of the Co impurity also increases along the ingot.

3.2. Dependences of galvanomagnetic parameters on tin concentration in alloys and temperature

It was found that in the entire temperature range studied, all samples are characterized by „metallic“ *p*-type conductivity (Figures 3, 4). At helium temperatures, as the tin concentration in the alloys increases, the resistivity ρ first rapidly decreases by about half and then almost does not change. The Hall coefficient R_H approximately doubles from the beginning to the middle of the ingot, and then decreases monotonously along the ingot. At the same time, the dependence of the Hall mobility $\mu_H = R_H/\rho$ on the concentration of tin in alloys has approximately the same form as the dependence $R_H(x)$, and the value of the Hall mobility reaches values $> 10^4\,cm^2/(V \cdot s)$, typical of $Pb_{1-x}Sn_xTe$ alloys with impurities of other 3*d* transition metals.

The most important result here is the presence of an extended area of decrease in the Hall coefficient, indicating a significant (by ~ 3 times) increase in the concentration of holes in the second half of the ingot. A similar Hall coefficient behavior was previously observed in previously studied $Pb_{1-x}Sn_xTe$ alloys with resonant levels of impurities in the valence band ($Pb_{1-x-y}Sn_xFe_yTe$ [26] and $Pb_{1-x-y}Sn_xNi_yTe$ [19]). It was considered one of the direct proofs of the existence of a resonant impurity level in the valence band and the stabilization (pinning) of the Fermi level by this level. The length of the Hall coefficient decline section is slightly different for us, but the general type of dependence is the same. Therefore, we also, as in the two previous cases, believe that the dependence $R_H(x)$ obtained by us indicates pinning of the Fermi level by the level of the Co impurity and the redistribution of electrons between the impurity level and the valence band with an increase in the tin content.

The temperature dependences of the resistivity and Hall mobility of holes in the studied samples, shown in Figures 4, *a* and *c*, have the form typical for degenerate semiconductors $A^{IV}B^{VI}$ under scattering charge carriers on ions and neutral impurity atoms at low temperatures and mainly on acoustic phonons in the high temperature range [26,29].

At the same time, the temperature dependences of the Hall coefficient show a significant (by 2−2.5 times) anomalous increase in the Hall coefficient, indicating a gradual decrease in the concentration of holes (Figure 4, *b*). This effect can be considered the second direct proof of the existence of a resonant impurity level of Co in the valence band. Then, as a result of an increase in the band gap and the convergence of the top of the valence band with the resonant level, as the temperature increases, electrons flow from the resonant level to the valence band and the concentration of holes in the valence band decreases. This effect was first detected in semiconductors $A^{IV}B^{VI}$ in a lead telluride with an impurity of In and was discussed in detail in Refs. [30,31]. Moreover, it was observed in a number of PbTe-based alloys with impurity levels of 3*d* transition metals located both in the conduction band [2,3,16] and in the valence band [19,25,26].

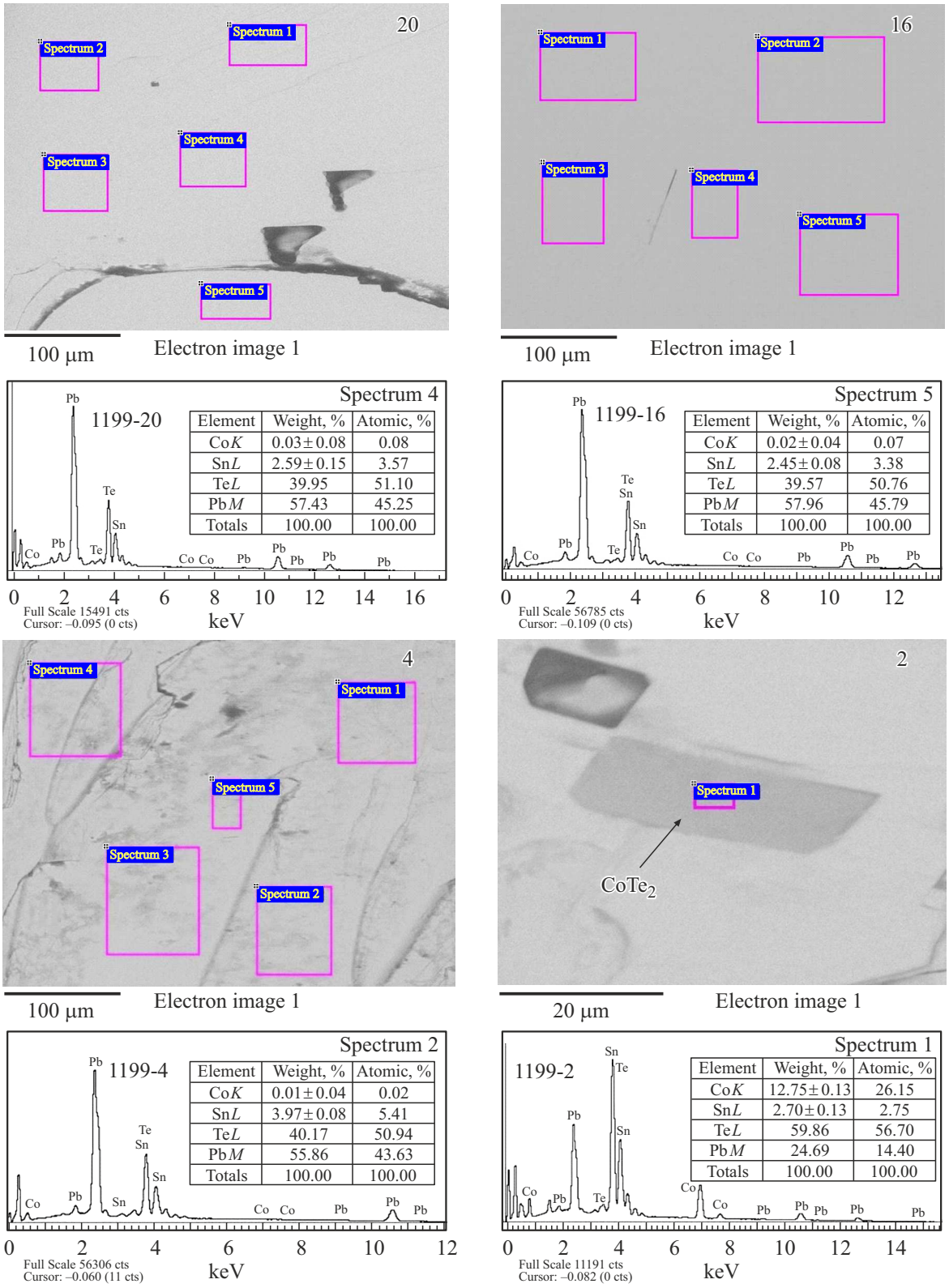

Figure 1. Photographs of the chipped surfaces and X-ray emission spectra for the areas indicated on them in samples 20, 16, 4 and 2.

3.3. Rearrangement of the electronic structure with change in alloy composition

The results of the study of the galvanomagnetic parameters of the $Pb_{1-x-y}Sn_xCo_yTe$ samples allowed constructing the dependences of the hole concentration p and the Fermi energy $(E_v - E_F)$ at $T = 4.2$ K of the tin content x. Similar calculations within the framework of the two-band dispersion law for semiconductors $A^{IV}B^{VI}$ [29] were previously performed by us when studying the electronic structure of alloys $Pb_{1-x}Sn_xTe$, doped with Cr, Fe, and Ni, and their main features are described in detail in Refs. [16,26].

The dependences obtained in this way for $Pb_{1-x-y}Sn_xCo_yTe$ alloys are represented by dots and solid lines in Figure 5. The dashed lines here also show the dependence of the position of the resonant levels of Fe and Ni and the concentration of holes on the tin content in alloys $Pb_{1-x-y}Sn_xFe_yTe$ [26] and $Pb_{1-x-y}Sn_xNi_yTe$ [19]. When constructing these lines, it was assumed that in a wide range of tin concentrations, pinning of the Fermi level is observed by impurity levels that move relative to the top of the valence band at a rate of $d(E_v - E_{Fe,Ni,Co})/dx \approx 7.3$ meV/mol %, obtained for alloys doped with Fe. The point is that in these alloys, results from studying samples from two ingots with tin concentrations in the range $x = 0.06-0.15$ and two different initial iron concentrations $y = 0.01$, 0.02 were used for this purpose, as well as the value of the Fe level energy in PbTe (i. e., at $x = 0$), which had been reliably established earlier [14]. Therefore, the area of linear growth of Fermi energy with increasing tin concentration, corresponding to the pinning range of the Fermi level with the impurity level, overlapped the widest range of compositions $x = 0-0.15$ and the accuracy of determining the slope angle when extrapolating experimental points to the dependence $(E_v - E_F)(x)$ with a straight line was maximum.

Comparison of the dependences shown in Figure 5 for $Pb_{1-x-y}Sn_xCo_yTe$ alloys with similar dependences for previously well-studied $Pb_{1-x-y}Sn_xFe_yTe$ alloys [26] shows that monotonous increases in Fermi energy and hole concentrations are observed only at tin concentrations $x = 0.10-0.13$. Most likely, this is due to the lower degree of solubility of the cobalt impurity and, as a result, a narrower range of matrix compositions, in which the effect of pinning the Fermi level in the samples studied by us is observed. Therefore, independent determination of the rate of movement of the Co level with a change in the matrix composition proved difficult and we used the above-mentioned composite coefficient of movement of the resonant level for linear approximation of the dependence $(E_v - E_F)(x)$, reliably established for Fe-doped alloys, in which pinning of the Fermi level was observed in wide ranges of matrix composition changes, almost coinciding with compositional coefficients of motion of Cr and V levels in $Pb_{1-x}Sn_xTe$ alloys [16,17]. It turned out that the resonant level of Co is located above the level of Fe and only slightly above the level of Ni. Extrapolation of the solid lines in Figure 5 to the value $x = 0$ shows that as the tin content decreases, the impurity level of Co approaches the top of the valence band, the hole concentration should decrease and go to zero, and in PbTe the Co level should be in the band gap.

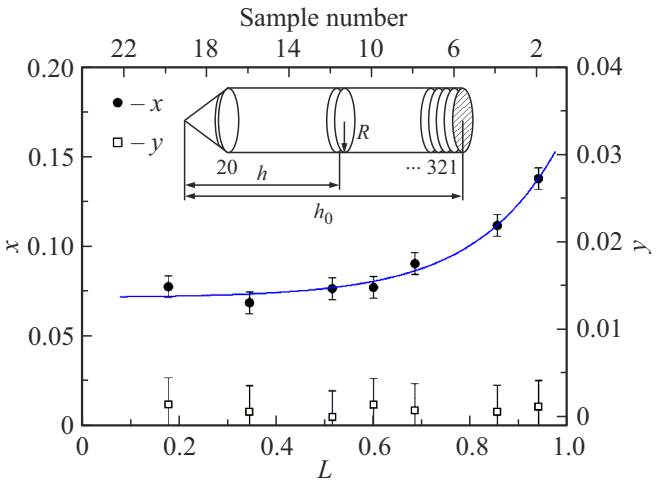

Figure 2. Distribution of tin and cobalt impurity along the ingot $Pb_{1-x-y}Sn_xCo_yTe$ ($L = h/h_0$ — relative coordinate of the washer in the ingot).

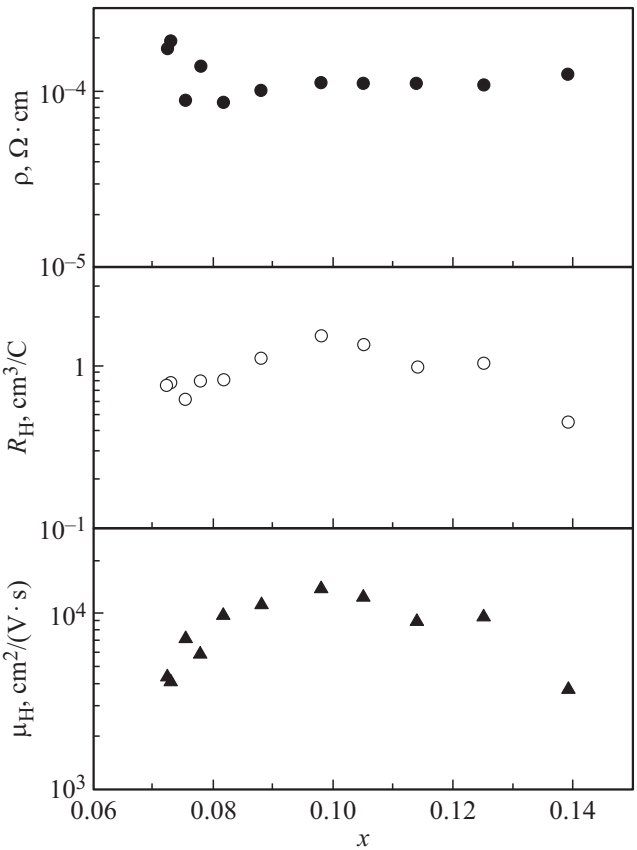

Figure 3. Dependences of resistivity, Hall coefficient, and Hall mobility at $T = 4.2$ K on the concentration of tin in alloys.

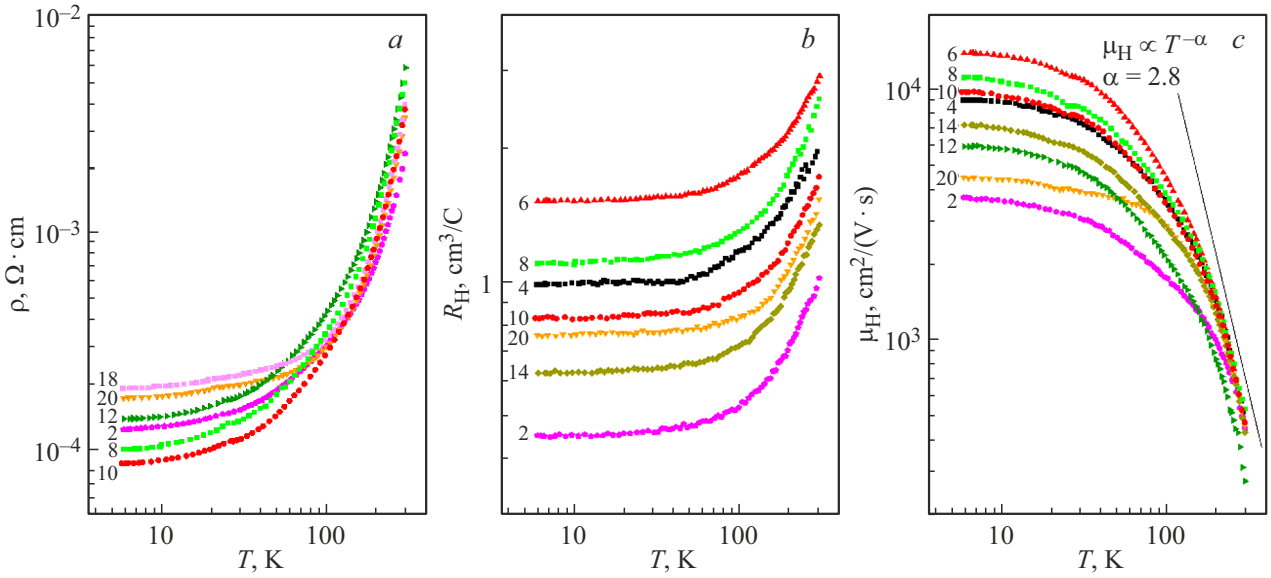

Figure 4. Temperature dependences of galvanomagnetic parameters $Pb_{1-x-y}Sn_xCo_yTe$ (curve numbers correspond to the sample numbers in the ingot).

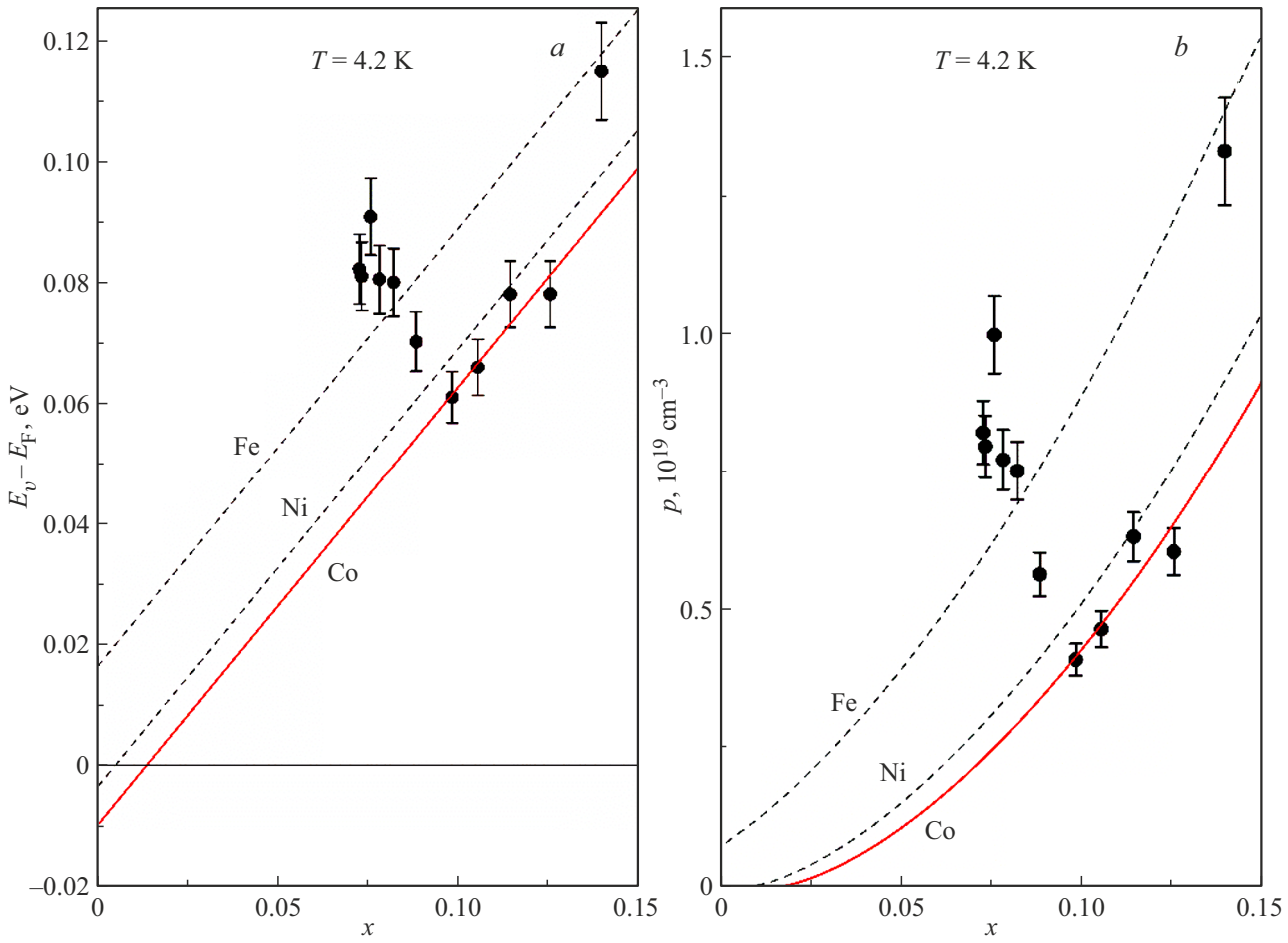

Figure 5. Dependences of the Fermi energy and hole concentration at $T = 4.2$ K on the tin concentration in alloys $Pb_{1-x-y}Sn_xCo_yTe$.

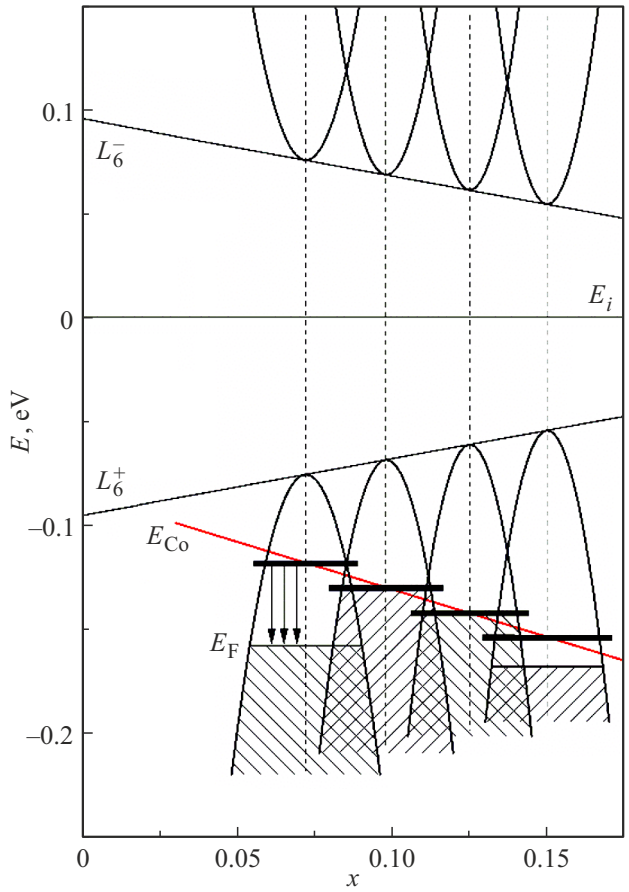

Figure 6. Diagram of the rearrangement of the electronic structure of $Pb_{1-x-y}Sn_xCo_yTe$ at $T = 4.2$ K with increasing concentrations of tin and cobalt impurity along the ingot.

The experimental and computational results shown in Figure 5 allowed constructing a diagram of the rearrangement of the electronic structure of alloys $Pb_{1-x-y}Sn_xCo_yTe$ ($x = 0.07-0.14$) at $T = 4.2$ K (Figure 6). As the concentrations of tin and cobalt impurity increase along the ingot, the band gap decreases, and the resonant level of Co, located at the beginning of the ingot above the Fermi level E_F, moves downward linearly, moving away from the top of the valence band at a rate of $d(E_v - E_{Co})/dx \approx 7.3$ meV/mol%. At the same time, the concentration of electron-filled states at the impurity level increases, and in the region from the beginning to the middle of the ingot, electrons from the Co level gradually fill the valence band. Therefore, there is a rapid decrease in the concentration of holes (see Figure 5), the movement of the Fermi level and the empty Co level towards each other and the pinning of the Fermi level by the resonant level. As the Co level continues to move down in energy, electrons are redistributed between the valence band and the impurity level (electrons flow from the valence band to the impurity level) and the concentration of holes in the valence band increases (see Figure 5). Finally, at the very end of the ingot, the mode of the pinning the Fermi level by the level of Co impurity is disrupted, the hole concentration is slightly higher than expected in the pinning mode, and the Fermi level is below the Co level (see Figure 5), which corresponds to the complete emptying of this level.

At first glance, the latest experimental result does not fit into the general scheme of the model described above, since, following its logic, one would rather expect a complete filling of the impurity level with electrons flowing from the valence band, as has already been observed in one of the ingots $Pb_{1-x-y}Sn_xFe_yTe$ [26]. Most likely, a violation of the pinning regime of the Fermi level and a sharp increase in the hole concentration are associated with a weakening of the donor effect of the Co impurity as a result of the formation of inclusions of the second phase enriched in Co, and, consequently, a slowdown in the growth or even a decrease in the impurity concentration in the main phase at the end of the ingot.

In addition, to provide a reasonable explanation of the nature of changes in the concentration of free charge carriers with increasing tin concentration in the alloys we studied $Pb_{1-x-y}Sn_xCo_yTe$, it is also necessary to have information about changes in the concentrations of intrinsic point defects (vacancies and interstitial atoms in sublattices of metal and chalcogen), providing a certain (electronic or hole) the type of conductivity and the concentration of free charge carriers in the undoped samples. Unfortunately, this information is missing almost always and in our case. However, it is well known that undoped PbTe is usually characterized by metallic conductivity of the *p*-type with a typical concentration of holes $(2-5) \cdot 10^{18}$ cm^{-3}, due to the predominant action of acceptor type defects (vacancies in the metal sublattice) [29]. As the concentration of tin in $Pb_{1-x}Sn_xTe$ alloys increases, the concentration of holes increases monotonously, presumably as a result of an increase in the concentration of these vacancies. This circumstance may also be the reason for a violation of the pinning regime of the Fermi level at the very end of the ingot.

It is also possible that for this reason, as well as due to the low solubility of impurities of 3*d* transition metals in none of the previously studied ingots of $Pb_{1-x}Sn_xTe$ doped with Cr, Fe and Ni, the pinning regime of the Fermi level by the resonant impurity level did not extend to the entire ingot and was disrupted in the samples either from the beginning or from the end of the ingot, and in our case, with low solubility of the Co impurity — both at the beginning and at the end of the ingot.

4. Conclusion

It is shown that the tin concentration increases exponentially along the ingot $Pb_{1-x-y}Sn_xCo_yTe$ ($x = 0.08$, $y = 0.01$), overlapping the range of compositions $x = 0.07-0.14$. In a number of samples, mainly from the end of the ingot, microscopic inclusions of the second phase were found, representing clearly defined regions with

a reduced content of Pb and Sn, but enriched in Co and Te (similar in composition to the compound $CoTe_2$).

Qualitative effects indicating pinning of the Fermi level by the resonant impurity level of Co in the valence band of $Pb_{1-x}Sn_xTe$ alloys have been found, and dependences of the Fermi energy and hole concentration at helium temperatures on the tin concentration have been obtained. Based on these calculations, it was found that the Co level is located slightly above the Ni level and the compositional coefficient of its movement relative to the top of the valence band band is estimated.

A diagram of the rearrangement of the electronic structure $Pb_{1-x-y}Sn_xCo_yTe$ with an increase in tin concentration along the ingot is constructed. It is shown that, unlike previously studied alloys with Cr, Fe, and Ni impurities, pinning of the Fermi level by the Co level is observed only in a narrow range of tin concentrations ($x = 0.10-0.13$). In samples up to the middle of the ingot and at its very end, the pinning mode is disrupted, and possible causes of this effect are discussed.

Funding

This study was performed under the state assignment of the M.V. Lomonosov Moscow State University.

Conflict of interest

The authors declare that they have no conflict of interest.

References

[1] V.V. Teterkin, F.F. Sizov, L.V. Prokofeva, Y.S. Gromovoi, M.N. Vinogradova. Sov. Phys. Semicond., **17**, 489 (1983).
[2] M. Ratuszek, M.J. Ratuszek. J. Phys. Chem. Solids, **46**, 837 (1985).
[3] V.D. Vulchev, L.D. Borisova. Phys. Status Solidi A, **99**, K53 (1987).
[4] B.A. Akimov, P.V. Verteletski, V.P. Zlomanov, L.I. Ryabova, O.I. Tananaeva, N.A. Shirokova. Sov. Phys. Semicond., **23**, 151 (1989).
[5] L.M. Kashirskaya, L.I. Ryabova, O.I. Tananaeva, N.A. Shirokova. Sov. Phys. Semicond., **24**, 848 (1990).
[6] E. Grodzicka, W. Dobrowolski, T. Story, Z. Wilamowski, B. Witkowska. Cryst. Res. Technol., **31**, S651 (1996).
[7] B.A. Volkov, L.I. Ryabova, D.R. Khokhlov. Phys. Usp., **45**, 819 (2002).
[8] *Lead Chalcogenides: Physics and Applications, Optoelectronic Properties of Semiconductors and Superlattices*, ed. by D.R. Khokhlov (N.Y.–London, Taylor and Francis, 2003) v. 183.
[9] A.A. Vinokurov, S.G. Dorofeev, O.I. Tananaeva, A.I. Artamkin, T.A. Kuznetsova, V.P. Zlomanov. Inorg. Mater., **42**, 1318 (2006).
[10] E.P. Skipetrov, L.A. Skipetrova, A.V. Knotko, E.I. Slyn'ko, V.E. Slyn'ko. J. Appl. Phys., **115**, 133702 (2014).
[11] J.D. König, M.D. Nielsen, Y. Gao, M. Winkler, A. Jacquot, H. Böttner, J.P. Heremans. Phys. Rev. B, **84**, 205126 (2011).
[12] E.P. Skipetrov, A.V. Knotko, E.I. Slynko, V.E. Slynko. Low Temp. Phys., **41**, 141 (2015).
[13] A.A. Vinokurov, A.I. Artamkin, S.G. Dorofeev, T.A. Kuznetsova, V.P. Zlomanov. Inorg. Mater., **44**, 576 (2008).
[14] E.P. Skipetrov, O.V. Kruleveckaya, L.A. Skipetrova, E.I. Slynko, V.E. Slynko. Appl. Phys. Lett., **105**, 022101 (2014).
[15] E.P. Skipetrov, B.B. Kovalev, I.V. Shevchenko, A.V. Knotko, V.E. Slynko. Semiconductors, **54**, 1171 (2020).
[16] E.P. Skipetrov, N.A. Pichugin, E.I. Slyn'ko, V.E. Slyn'ko. Low Temp. Phys., **37**, 210 (2011).
[17] E.P. Skipetrov, A.N. Golovanov, A.V. Knotko, E.I. Slyn'ko, V.E. Slyn'ko. Semiconductors, **46**, 741 (2012).
[18] E.P. Skipetrov, B.B. Kovalev, L.A. Skipetrova, A.V. Knotko, V.E. Slynko. J. Alloys Compd., **775**, 769 (2019).
[19] E.P. Skipetrov, N.S. Konstantinov, E.V. Bogdanov, A.V. Knotko, V.E. Slynko. Low Temp. Phys., **47**, 24 (2021).
[20] J.P. Heremans, V. Jovovich, E.S. Toberer, A. Saramat, K. Kurosaki, A. Charoenphakdee, S. Yamanaka, G.J. Snyder. Science, **321**, 554 (2008).
[21] J.P. Heremans, B. Wiendlocha, A.M. Chamoire. Energy Environ. Sci., **5**, 5510 (2012).
[22] B. Wiendlocha. Phys. Rev. B, **97**, 205203 (2018).
[23] T. Parashchuk, B. Wiendlocha, O. Cherniushok, R. Knura, K.T. Wojciechowski. ACS Appl. Mater. Interfaces, **13**, 49027 (2021).
[24] K.A. Kikoin, V.N. Fleurov. Transition Metal Impurities in Semiconductors: Electronic Structure and Physical Properties, World Scientific, Singapore (1994).
[25] E.P. Skipetrov, O.V. Kruleveckaya, L.A. Skipetrova, A.V. Knotko, E.I. Slynko, V.E. Slynko. J. Appl. Phys., **118**, 195701 (2015).
[26] E.P. Skipetrov, B.B. Kovalev, L.A. Skipetrova, A.V. Knotko, V.E. Slynko. Low Temp. Phys., **45**, 201 (2019).
[27] V.E. Slynko, W. Dobrowolski. Bull. Natl. University „Lviv Polytechnic", Electronica, No. 681, 144 (2010).
[28] E.I. Slynko, V.M. Vodopyanov, A.P. Bakhtinov, V.I. Ivanov, V.E. Slynko, W. Dobrowolski, V. Domukhowski. Visn. Lviv Polytec. Natl. Univ., Electronica, No. 734, 67 (2012).
[29] G. Nimtz, B. Schlicht. In: *Narrow-Gap Semiconductors, Springer Tracts in Modern Physics* (Berlin–Heidelberg–N.Y.–Tokyo, Springer, 1983) v. 98, p. 1.
[30] V.I. Kaidanov, Yu.I. Ravich. Phys. Usp., **28**, 31 (1985).
[31] S. Nemov, M. Auslender, R. Shneck, Z. Dashevsky. In: *Advanced Thermoelectric Materials — Theory, Development, and Applications, ed. by Uday Basheer Al-Naib* (IntechOpen, 2025) chapter 4.

Translated by A.Akhtyamov